VALIDATION OF A WAVE ENERGY CONVERTER NUMERICAL MODEL THROUGH SMALL SCALE LABORATORY MEASUREMENTS

Lilia CARLO[(*)], Sebastian BRUSCA[(*)], Filippo CUCINOTTA[(*)],
Antonio GALVAGNO[(*)], Carla FARACI[(*)] & Felice ARENA[(**)]

[(*)]*University of Messina, Department of Engineering, Contrada di Dio, Villaggio S. Agata, Messina 98166, Italy.*
[(**)]*Mediterranea University of Reggio Calabria, DICEAM Department, Via Graziella Feo di Vito, 89122 Reggio Calabria, Italy.*
Corresponding author: lcarlo@unime.it

EXTENDED ABSTRACT

A seguito della presa di coscienza delle problematiche relative al consumo energetico da fonti non rinnovabili, come i combustibili fossili, l'attenzione verso fonti di energia rinnovabile è cresciuta sensibilmente. Finora, le fonti energetiche rinnovabili più sfruttate sono state l'energia solare, eolica e geotermica. Tuttavia, negli ultimi anni, l'energia del moto ondoso ha attirato grande attenzione grazie alla sua elevata densità energetica e la sua ampia diponibilità globale. A tal proposito, la ricerca ha soffermato l'attenzione sui dispositivi di conversione di energia, comunemente definiti WEC (Wave Energy Converter), che permettono di trasformare l'energia potenziale e cinetica di un'onda in energia elettrica. Tali dispositivi sono classificati secondo il principio di funzionamento, la posizione rispetto al fronte d'onda, la posizione rispetto alla costa e le dimensioni. Tra i dispositivi WEC quelli più comunemente utilizzati sono i sistemi a colonna d'acqua oscillante OWC e i dispositivi U-OWC (o REWEC), dotati di un condotto a U sul lato battuto dalle onde (Boccotti, 2002), e sistemi basati sul funzionamento ad overtopping (Vicinanza *et alii*, 2014).

Il sistema OWC, diffuso per la sua efficienza energetica, la facilità costruttiva e il ridotto impatto ambientale, consiste in una camera d'aria semi-sommersa collegata all'atmosfera mediante un condotto contenente una turbina, e collegato al mare mediante un'apertura posta sotto la superficie libera. L'oscillazione del pelo libero, prodotto dal moto ondoso, determina una compressione e decompressione dell'aria al suo interno, generando un flusso bidirezionale che muove la turbina. L'andamento dei flussi di aria e d'acqua all'interno dei dispositivi OWC è fortemente influenzato dalle caratteristiche geometriche del cassone e dalle condizioni dell'onda incidente. Pertanto studiare separatamente tali fenomeni non permette di comprendere al meglio il funzionamento complessivo del sistema. Un attento studio globale è stato condotto da Boccotti (2007), il quale introduce il concetto di periodo proprio di oscillazione della colonna d'acqua, dimostrando che sotto l'azione di stati di mare generati dal vento e di onde di mare lungo, i dispositivi U-OWC grazie alla presenza del condotto verticale ad U, raggiungono condizioni di risonanza. Il miglioramento delle prestazioni di un dispositivo U-OWC è dovuto, inoltre, alle maggiori ampiezze delle fluttuazioni di pressione all'imboccatura.

Il principale obiettivo del presente lavoro è stato implementare un modello di analisi fluidodinamica computazionale (CFD), mediante il codice di calcolo Ansys Fluent. Il modello numerico è stato validato mediante una campagna sperimentale condotta in piccola scala, realizzata all'interno di una canaletta dotata di generatore d'onde a pistone e di un dispositivo U-OWC, riproduzione in scala del cassone REWEC installato nel laboratorio NOEL di Reggio Calabria. L'apparato sperimentale, implementato nel Software di CFD, è un dominio rettangolare 2D che risolve il campo di moto attraverso le Reynolds-Averaged Navier-Stokes (RANS) Equations; l'insieme di tali equazioni differenziali parziali viene risolto con il Metodo dei Volumi Finiti (FVM). L'approccio numerico ha previsto l'utilizzo di un modello VOF (Volume Of Fluid) per l'interazione aria-acqua e un modello k - ω per tenere conto degli effetti della turbolenza.

Il modello è stato validato mediante il confronto delle misure numeriche e sperimentali delle oscillazione del pelo libero. Per mezzo di una fotocamera rapida, è stato possibile acquisire le immagini sperimentali relative alla superficie libera sia all'interno della canaletta sia all'interno del condotto verticale dell'U-OWC. Elaborando le immagini mediante un algoritmo implementato sul Software Matlab, si sono confrontate le misure sperimentali e le misure numeriche estrapolate dal modello.

Infine, il modello numerico validato è stato utilizzato per eseguire un'analisi del bilancio energetico del cassone al variare dei parametri dell'onda incidente, altezza e frequenza dell'onda, ed al variare delle caratteristiche geometriche del dispositivo U-OWC, altezza e lunghezza della camera d'aria. I risultati ottenuti dal bilancio energetico costituiscono un valido strumento per definire la forma e le dimensioni ottimali da adottare nelle future campagne sperimentali e numeriche, al fine di massimizzare la produzione energetica del dispositivo e ridurre al minimo le perdite dovute alla formazione di vortici.

ABSTRACT

In the field of Engineering, research has conveniently exploited the fluids for energy production. The possibility to use marine renewable energy is still under development, in particular, among the wave energy converter devices the U-OWC systems are the most promising.

The main objective of this work is to validate a numerical model with an experimental campaign that aims to simulate the flow field in front of the breakwater and inside the U-OWC. The tests were carried out to understand the hydrodynamic behaviour of the device in regular wave conditions, inside a flume with rectangular section, equipped by a piston-type wave-maker and a U-OWC device, reproducing the REWEC caisson installed in the Natural Ocean Engineering Laboratory (NOEL) of Reggio Calabria, with a 1:13.5 scale. Measurements of the water free surface were used exclusively to validate the 2D numerical model developed through the Ansys Fluent Computational Fluid-Dynamics (CFD) Software.

The numerical model solves the fluid flow field using the RANS equations, in which the air-water interaction governed by this set of partial difference equations is solved with the Finite Volume Method (FVM).

In conclusion, results related to the energy efficiency of the caisson were extrapolated from the validated numerical model.

KEYWORDS: Computational Fluid Dynamics, U-OWC, wave energy, image analysis.

INTRODUCTION

In the last thirty years, the focus on environmental protection, combined with the exhaustion of fossil fuel reserves, led to a growing interest in renewable, alternative and ecological energy resources. Today, innumerable technologies have been developed to exploit renewable energy resources, such as solar, wind or hydroelectric ones.

The most recent challenge in the energy field is the development of technologies able to exploit marine energy (DREW *et alii*, 2009). Oceans and seas cover 70% of the earth's surface and therefore constitute a huge source of energy for the satisfaction of the energy needs of the whole world.

Among the most advanced technologies that allowed the exploitation of wave energy there are the Wave Energy Converters (WEC) devices. Over the years, a variety of techniques of WEC systems were developed, allowing to convert the energy contained in the waves into electricity energy. These techniques can be classified according to their location, size and working principle (LOPEZ *et alii*, 2013). According to working principle classification, the wave energy converters can be classified in oscillating water column devices (OWC) (FALCÃO & HENRIQUES, 2015, KO *et alii*, 2017), overtopping devices (VICINANZA *et alii*,

2014, CONTESTABILE et *et alii*, 2017) and oscillating devices (FALCÃO, 2010, LIANG & ZUO, 2017).

The OWC system is a semi-submerged air chamber connected to the atmosphere by a duct containing a turbine, and connected to the sea by an opening under the free surface. The oscillation of the free surface, produced by the wave motion, determines a compression and decompression of the air inside it, generating a bidirectional flow that moves the turbine.

The OWC systems are among the simplest WEC devices from the constructive and maintenance point of view. They can be deployed as fixed structures at the shoreline or nearshore, or integrated into floating structures (FALCÃO & HENRIQUES, 2015) and in breakwater ports (NATY *et alii*, 2016).

In 2002 BOCCOTTI patented a new OWC device called REWEC1, a modular structure made with prefabricated caissons placed side by side, in order to form a submerged breakwater having the dual purpose to defend the coast and to produce electricity through generators connected to turbines (Well type).

The substantial difference between a REWEC device and a conventional OWC lies in the presence of a U-shaped duct, which connects the water column with the external flow field. In 2007 BOCCOTTI introduced the concept of the proper period of oscillation of the water column, demonstrating that under the action of sea states generated by wind and long sea waves, U-OWC devices reach resonance conditions, improving their performance.

Oscillating Water Column (OWC) devices are among the most tested WECs, both analytically (MALARA *et alii*, 2017), experimentally (BRUSCA *et alii*, 2015; SCARPETTA *et alii*, 2017) and numerically (FILIANOTI *et alii*, 2008). The numerical model of OWC devices and their interaction with the waves can be a very effective tool, as it is possible to verify the characteristics of the system virtually in different scenarios, without the need to build scaled prototypes or install them on site, saving time and money.

In general, there are two categories of numerical models, the first category, less effective in solving problems characterized by strong non-linearity, turbulence and complex viscosity, is based on the potential flow theory and is generally solved with the boundary element method (BEM) (BAUDRY *et alii*, 2013), the second category, more effective, is based on the Reynold-Averaged Navier-Stokes equations (RANS). Several authors have developed numerical models that solve the flow field with RANS equations, an example is ZHANG *et alii* (2012) who validated a 2D OWC numerical model and studied its performance with varying geometric parameters.

Another important 2D numeric model has been implemented by LUO *et alii* (2014) on the computational fluid dynamics code (Fluent), to investigate the effects of non-linearity of waves on an OWC device. The effects due to walls extending deeply in

the water were studied, evaluating the increase in reflection in regular and irregular wave conditions. A similar study was done by Simonetti *et alii* (2015), in which the OWC numerical model was implemented on the CFD OpenFoam code and was validated with the OWC device tested by Crema *et alii* (2015).

The main objective of this study was to validate a 2D numerical model through an experimental campaign conducted on a small scale, carried out inside a channel equipped with a piston type wave-maker and a U-OWC device, which is a scaled reproduction of the REWEC system installed in the NOEL laboratory in Reggio Calabria. The CFD numerical model, implemented on the Ansys Fluent Software, solves the fluid flow field through the Reynolds-Averaged-Navier-Stokes equations (RANS); with a VOF surface capturing scheme introduced by Hirt & Nichols (1981).

Additionally, the validated numerical model was used to perform an analysis of the device's energy balance as the parameters of the incident wave (height and period) and the geometric characteristics of the U-OWC device (length and height of air chamber) change.

Results concerning the energy efficiency, air pressure inside the chamber and chamber free surface elevation were extrapolated to obtain the optimal caisson dimensions to be implemented in a forthcoming large-scale experimental campaign. The validated numerical model is a valid tool to solve design problems and to look for the most suitable shape of the U-OWC duct, in order to maximize the energy production of the device and reduce the formation of vortices within the U-OWC.

NUMERICAL MODEL
Governing equation
In the present study, the numerical model is based on a CFD simulation using the Ansys Fluent Code. The model solves the fluid flow field using RANS (Reynold-Averaged Navier-Stokes) equations, in which this set of partial differential equations is solved with the Finite Volume Method (FVM).

The mass conservation equation for an incompressible flow

$$\frac{\partial \rho}{\partial t} + \frac{\partial}{\partial x_i}(\rho v_i) = 0 \tag{1}$$

and the equation of conservation of momentum is:

$$\frac{\partial \rho}{\partial t}(\rho v_i) + \frac{\partial}{\partial x_j}(\rho v_i v_j) =$$
$$= -\frac{\partial p}{\partial x_i} + \frac{\partial}{\partial x_i}\left[v\left(\frac{\partial v_i}{\partial x_j} + \frac{\partial v_j}{\partial x_i}\right)\right] + \frac{\partial}{\partial x_j}\left(-\overline{v_i' v_j'}\right) \tag{2}$$

where ρ is the mass density of the fluid, v_i is the time-averaged velocity vector, p is the pressure and v is the kinematic velocity.

Computational domain
The implemented numerical model is a 2D rectangular domain 2 m long. It represents a flume equipped with a piston-type wave-maker placed in the left extremity and a U-OWC device in the right extremity. The geometric dimensions of the breakwater are shown in Fig. 1. The distance between the wave-maker and the caisson is 1350 mm and the water depth is 123 mm.
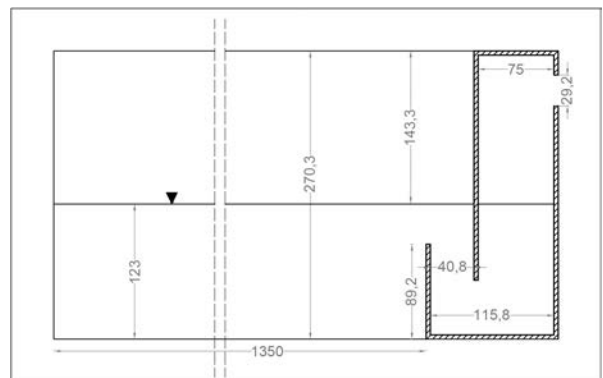

Fig. 1 - Scheme of the computational domain of the wave flume (measures are in millimetres).

The discretization of the domain was carried out using the PointWise Software, adopting a structured mesh with rectangular elements. The cell sizes are in the order of $dx = 0.0036$ m and $dy = 0.007$ m. The grid in the area of the free surface and in the area of the caisson was thickened to get more accurate results, with value of cell sizes of $dx = 0.0036$ m and $dy = 0.0015$ m and $dx = 0.0015$ m and $dy = 0.001$ m respectively (Fig. 2). The total mesh consists of 40.000 cells.
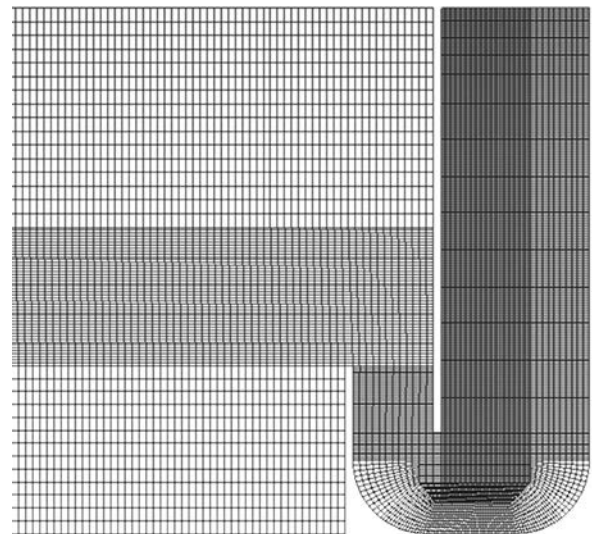

Fig. 2 - A detail of the grid mesh of the computation domain.

The boundary conditions implemented in the present CFD model are set as: no slip wall for the all solid walls (U-OWC and bottom), and pressure outlet for the top boundary of the domain (atmosphere) with zero gauge pressure.

The wave generation process is simulated by assigning a certain velocity using a user defined function (UDF) to the left wall, with a sinusoidal law (see Eq. 5). A dynamic mesh was assigned for both the left wall of the domain and the deformation of the neighbouring cells. GALVIN (1964) in his theory of generation wave from wave-maker defined the equation of transfer function for the wave paddle of a piston type wave-maker:

$$\frac{H}{S} = \frac{2(\cosh 2kh - 1)}{\sinh 2kh + 2kh} \tag{3}$$

where H is the wave height, S is the displacement of wave-maker, h is the water depth and k is the number wave. The displacement and velocity of wave-maker are given by the following equations:

$$x(t) = \frac{S}{2}\sin(\omega t) \tag{4}$$

$$v(t) = \frac{S}{2}\omega\cos(\omega t) \tag{5}$$

As before mentioned equation (5) was used to assign a velocity to the wave-maker, according to characteristics of incident wave. The presence of the turbine is taken into account by the implementation of a "porous zone" in order to model the pressure difference between the inside air chamber pressure and atmospheric pressure (MOÑINO *et alii*, 2017).

Numerical setting
The numerical model solve the Navier-Stokes equation for unsteady two-phase flow. The air and water interaction is taken into account by means the Euler-Euler approach. In particular, the VOF model is used to model the two-phase interaction, in which the volume of a phase is calculated as a volume fraction. The volume fraction of ith fluid occupying cells of the computational domain is calculated as:

$$\frac{\partial \alpha_i}{\partial t} + \nabla(\alpha_i v_i) = 0 \tag{6}$$

where α_i is an index that varies between 0 and 1, it is equal to 1 when the cell is full of fluid, it is equal to 0 when it is empty (FERREIRA *et alii*, 2015).
The volume fraction of the cells near the interface of the two phases is calculated using the Geometric Reconstruction scheme, in its explicit formulation to avoid excessive numerical dissipation. The interface is represented through a piecewise-linear interpolation. The air is assumed as compressible fluid, in order to take into account the compressibility of the air pocket inside the chamber, while water is assumed as incompressible fluid. A pressure-based solver is adopted for the discretization of the continuity and momentum equations.
The SIMPLE algorithm (Semi-Implicit Method for Pressure Linked Equations) is used to obtain the pressure field. The Green-Gauss cell based scheme is used for gradient, in order to discretize spatially the governing equations. The PRESTO! (Pressure Staggering Option) scheme is set for pressure equation, the Second Order Upwind is set for momentum equation and the First Order Implicit is set for the transient formulation. The two equations Shear-Stress-Transport (SST) k - ω turbulence model is assumed to take into account the Reynolds stresses and to mathematically close the problem. Regarding the temporal discretization, a *T/100* time step is used with 60 iterations for each time step, where T is the wave period.

EXPERIMENTAL SET UP
The numerical model used in the present study was validated thanks to a small-scale experimental campaign that was carried out within a plexiglass flume 2 m long with a rectangular cross section 0.1 x 0.2 m (Fig. 3a), equipped with a piston-type wave maker and a U-OWC device, reproducing the REWEC caisson installed in the Natural Ocean Engineering Laboratory (NOEL) of Reggio Calabria with a 1:13.5 scale.
The wave maker was made with a double-plate plexiglass piston, 250 mm high, 98 mm wide and 4 mm thick, placed inside the channel. In order to prevent the passage of water between the piston and the flume walls, a sheet of expanded polypropylene, larger than the plates, was inserted between one plate and another. To generate the waves an Arduino board series equipped by a micro-controller was used, generating the same wave train as the numerical model.

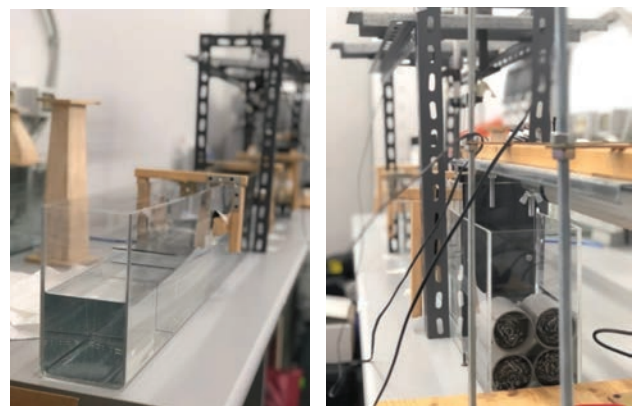Four absorbers were placed behind the piston, with the function of damping reflected waves (Fig. 3b). They were made

Fig. 3 - The experimental set up. a) plexiglass flume, b) absorbers.

with 50 mm diameter tubes inside which steel meshes have been inserted to dissipate the energy.

The U-OWC was made in ABS material, with a base area of 0.1x0.2 m and a height of 0.27 m. The device was inserted tightly inside the channel so that the water does not filter laterally. One of the faces of the caisson was made in plexiglass in order to make the oscillation of the free surface inside it visible (Fig. 4).

Fig. 4 - *U-OWC device in ABS and plexiglass materials of the experimental set up.*

Images of free surface, were acquired by means of a Phantom 1 Megapixel v711 rapid camera in order to reconstruct waves in the space and time domain. The camera allows to reach 7530 frames per second at a maximum resolution of 1280x800. In this study, the camera was set at maximum resolution and at a speed of 100 fps, with an exposure time of 3000 μs.

The camera was positioned so that its focal plane was parallel to the wall of the channel and able to focus at a useful length of over 300 mm. To improve the contrast, in order to better define the wave profile, a sheet of black cardboard was leant the back wall of the canal, while, to have an uniform reflection without unwanted objects, such as to avoid excessive disturbances to the image quality, a white cloth was placed in the area behind the camera.

VALIDATION PROCEDURE

Experimental tests were carried out at different wave frequencies and wave heights for the validation of the numerical model. For each test, a number of frames equal to 2000 were obtained, using the VirtualDub Software, allowed the conversion of video to frames. After converting the image to black and white, it was processed by implementing the Canny algorithm, a contour recognition operator to identify the wave profile on the Matlab Software.

In order to analyze both space and time domains, a space-time cubic matrix was created containing spatial elements, identified by

x and y coordinates, and time elements, identified by the number of frames. Pixels were converted to mm to obtain measurements in the International Length System.

The matrix has been cut in spatial terms at a fixed time to observe the points that identify the free surface. Subsequently, the points obtained were interpolated using the Fourier series of the third order, obtaining what is shown in Fig. 5.
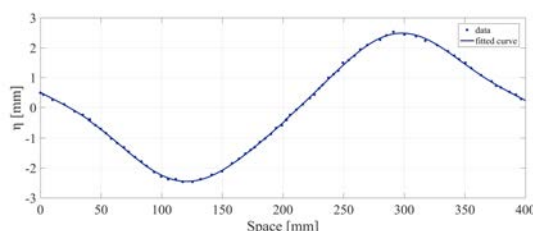

Fig. 5 - *Wave profile in space.*

In addition, the reverse operation was performed, i.e. a time cut of the matrix was made to a fixed space, so it was possible to observe the representative points of the wave propagation over time. The points obtained were interpolated using the Fourier series of the third order, as shown in Fig 6.
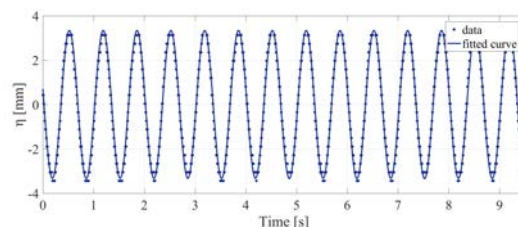

Fig. 6 - *Wave profile in time.*

From the frame analysis, experimental measurements of the oscillation of free surface η were performed both within the vertical duct of the U-OWC and inside the flume. These measurements were compared with the numerical measurements of the oscillation of free surface, extracted from the numerical model implemented on Ansys Fluent.

Figures 7 - 8 show the comparison in the time domain between the numerical and experimental measurements of the oscillation of free surface η, at a wave period of $T = 1$ s and at a wave height of $H = 0.0012$ m.

In Fig. 7, the measurements were carried out at a distance of 800 mm from the wave-maker, while in Fig. 8 the measurements were carried out within the caisson chamber.

Figures 7 - 8 show a good agreement with deviation of about 6% between numerical and experimental results for the free surface oscillation within the flume and of about 4% inside the U-OWC chamber, thus the wave troughs are a little bit underestimated by the numerical model.
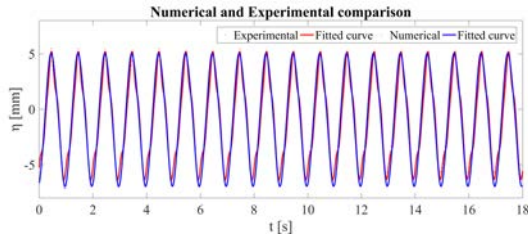
Fig. 7 - *Experimental and Numerical comparison free surface oscillation η at a distance of 800 mm from the piston, with wave period T = 1 s and wave height H = 0.012 m.*
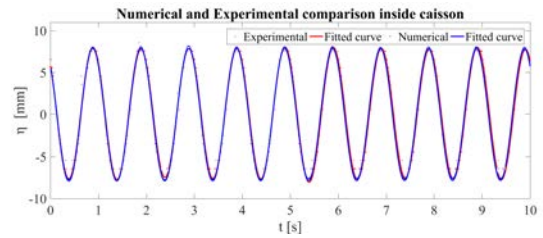

Fig. 8 - *Experimental and Numerical comparison free surface oscillation η inside the U-OWC, with wave period T = 1 s and wave height H = 0.012 m.*

ENERGY BALANCE ANALYSIS

An energy balance analysis of the U-OWC was performed, based on the Equation (7) (TSENG *et alii*, 2000):

$$E_I = E_R + E_E + E_S + E_L \left[\frac{J}{m}\right] \tag{7}$$

where E_I is the incident wave energy, E_R is the reflected wave energy, EE is the extracted energy, E_S is the potential energy and E_L is the energy losses.

From the linear wave theory (DEAN & DALRYMPE, 1992), the total energy per wave unit is expressed as:

$$E_I = \frac{1}{8}\rho g H^2 L \left[\frac{J}{m}\right] \tag{8}$$

where ρ is the water density, g is the gravitational acceleration, H is the wave height and L is the wave length.

While some of the incident wave energy is reflected by the U-OWC device, the rest is absorbed by the caisson (E_A), so the maximum energy that can be extract from the device is given as:

$$E_A = E_I - E_R = E_E + E_S + E_L \left[\frac{J}{m}\right] \tag{9}$$

The reflected wave energy E_R is expressed by the product between incident wave energy E_I and the square of reflection coefficient C_r. In general, in physical modeling the reflection coefficient can be evaluated through the known methods of the two probes (GODA & SUZUKI, 1976) and the three probes (MANSARD & FUNKE, 1980), or the more recent four-probe method (FARACI *et alii*, 2015; LIU & FARACI, 2014). In this study, the reflection coefficient was found by the three wave probe method of MANSARD & FUNKE (1980).

In the physical model, as the wave maker is not equipped with an active absorption system, the wave reflection is dampened by a sponge system at the back of the wave maker; instead in the numerical model such dampening is not taken into account, thus leading to results slightly overestimated for what concerns the reflected energy and underestimated for the energy absorbed by the caisson.

The extracted energy E_E from the PTO (Power Take Off) system

is given as the time integral of the product of total pressure difference between the inside and outside of the air chamber and the air flow rate across the PTO:

$$E_E = \int_0^T \Delta P(t) \cdot q(t) dt \left[\frac{J}{m}\right] \tag{10}$$

The U-OWC potential energy depends on the oscillation of free surface inside it and can be expressed as:

$$E_S = \frac{1}{16}\rho g H_W^2 b \left[\frac{J}{m}\right] \tag{11}$$

where H_W is the height of the water column oscillation inside the U-OWC's chamber and b is the chamber length.

From the energy conservation principle in Eq. (7), the total energy lost as a result of viscosity, turbulence and vortex is given as:

$$E_L = E_A - E_S - E_E \left[\frac{J}{m}\right] \tag{12}$$

RESULTS AND DISCUSSION

The validated model was used to carry out an analysis of the energy balance as the characteristics of the incident wave and the geometric parameters of the U-OWC's air chamber varied.

A first analysis was conducted to get the C_r reflection coefficient as the wave period T varied keeping fixed the wave height H (Case A), and a second analysis as the wave height H varied keeping the wave period T fixed (Case B).

Case A	T (s)	Cr
H= 0.012 m	0.67	0.7105
	0.56	0.7192
	0.50	0.7688
Case B	**H (m)**	**Cr**
T = 0.67 s	0.010	0.7173
	0.012	0.7105
	0.014	0.7263

Tab. 1 - *Results of reflection coefficient at different wave height (Case A), and different wave period (Case B).*
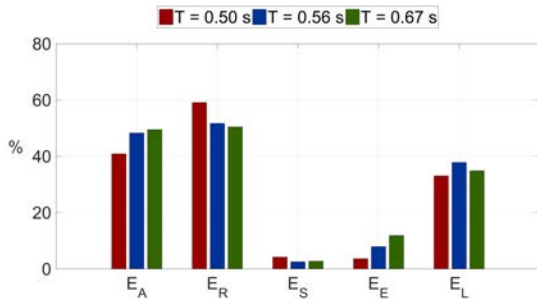
Fig. 9 - Comparison between energy balances for three different wave periods at a wave heights of H = 0.012 m (Case A).
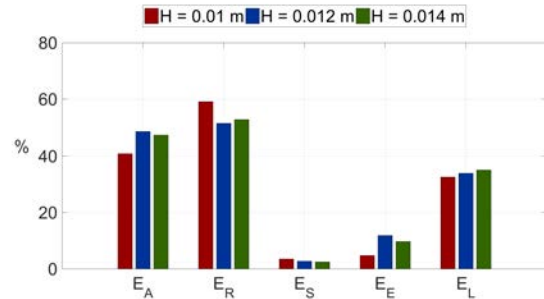

Fig. 10 - Comparison between energy balances for three different wave heights at a wave period of T = 0.67 s (Case B).

The reflection coefficient was obtained using the method of the three probes (MANSARD & FUNKE, 1980), the results are summarized in Table 1.

In both Cases A - B, the tests exhibit similar hydrodynamic performances. However, the reflection coefficient tends to increase as the wave period decreases and it is higher for values of $H = 0.012$ m.

From the reflection results, it was possible to carry out an analysis of the energy balance. Figure 9 shows the results of energy components of the energy conservation equation (Eq. 7), for three different wave periods at the same wave height $H = 0.012$ m (Case A). It can be seen that the reflected energy (E_R) increases as the wave period decreases, with a maximum of 59% for wave period of $T = 0.5$ s, also, an increase of the extracted energy (E_E) with the increase of the wave period, with a maximum value of $E_E = 12\%$ for $T = 0.67$ s.

Figure 10 shows an increase in reflected energy (E_R) and a decrease in absorbed energy (E_A) as the wave height increases, however, this trend is not respected for the wave height values of $H = 0.01$ m. The energy losses (E_L) increase with the increase in wave height, with $E_L = 38\%$ for wave height of $H = 0.014$ m.

The extracted energy (E_E) from the U-OWC device is maximum for $H = 0.012$ m values with percentages that reach 11%.

From the comparison of the energy results analyzed in the cases shown in Figs. 9 - 10, the maximum energy efficiency in terms of extracted energy (E_E) from the PTO system is reached under the conditions of the wave period of $T = 0.67$ s, and wave height of $H = 0.012$ m. For this reason, the characteristics of the incident wave remained the same in the subsequent analysis of the performance device.

From the results obtained so far, as the parameters of the incident wave vary, there are enormous energy losses (E_L) and small amounts of energy extracted (E_E) from the PTO system. The geometric parameters of the caisson were changed to improve the efficiency of the U-OWC device, in order to reduce the energy losses 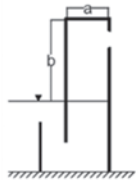and to increase the extracted energy. By maintaining the wave parameters unvaried, the effect of the dimension of the caisson's chamber on the performance of the U-OWC system is studied by varying the length (a) and the height (b) of the air chamber. Indeed, the resonant behaviour of the caisson is strongly influenced by changing the geometric dimensions of the chamber because the normal period of the system varies. For this reason, three different cases are considered varying 'a' and three different cases are considered varying 'b' represented in a non-dimensional form as follows in Table. 2, being k the wave number.

The above tests are executed in the numerical flume for the wave characteristics of $H = 0.012$ m, $T = 0.67$ s. Figure 11 shows the instantaneous chamber free surface oscillation η, air pressure oscillation Δp, airflow rate q and extracted power P_E from PTO system in the three different cases where ka varies (Table 2).

As expected, the free surface oscillation η increases as the length of the air chamber (ka) decreases, causing increasing pressure fluctuations, as it is observed passing from case (i) to case (iii). This result translates into an increase in extracted power from the PTO system.

For values of $ka = 0.449$, the wave height reaches values of $H_w = 0.011$ m within the vertical duct and amounts of extracted power of about $P_E = 0.12$ J/s. This is due to a small increase in pressure during the outlet air phase in comparison to the inlet air phase.

Figure 12 shows the results obtained when the height of the air chamber changes in the three cases analyzed. Compared to the previous case, in which the wave height grew with the shortening of the air chamber, there is a smaller increase in wave height as kb values increase. This involves smaller potential energy values E_S.

	(i)	(ii)	(iii)	
	0.673	0.561	0.449	ka
	1.286	1.072	0.857	kb

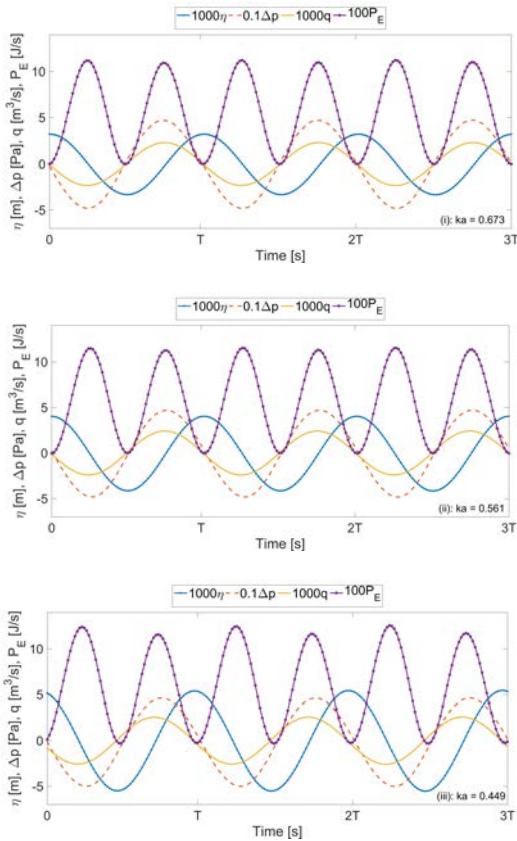*Tab. 2 - Scheme of tests performed at different values of ka and kb.*

Fig. 11 - Instantaneous chamber free surface oscillation η, air pressure oscillation Δp, airflow rate q and extracted power P_E with T = 0.67 s and H = 0.012 m. i) ka = 0.673, ii) ka = 0.561, iii) ka = 0.449.
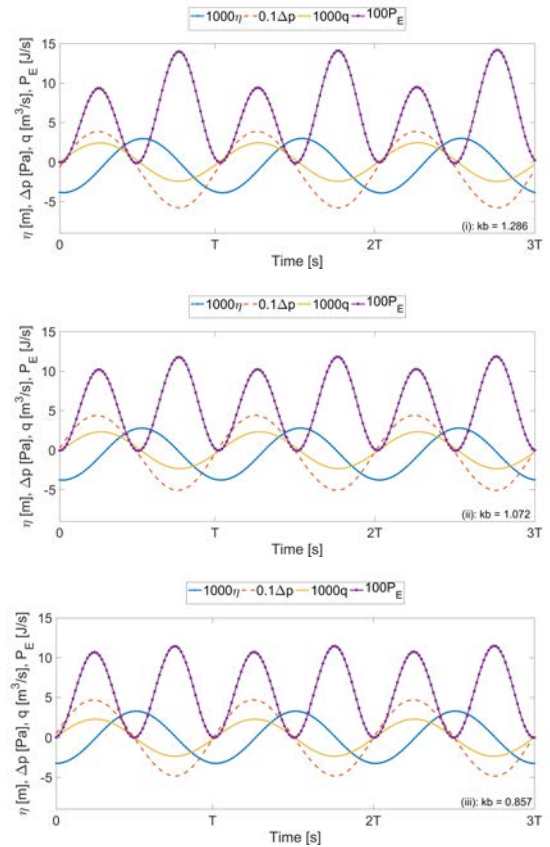

Fig. 12 - Instantaneous chamber free surface oscillation η, air pressure oscillation Δp, airflow rate q and extracted power P_E with T = 0.67 s and H = 0.012 m. i) kb = 1.286, ii) kb = 1.072, iii) kb = 0.857.

Comparing Fig 12i and 12iii, the main difference is seen in the trend of the extracted power, in fact, while in Fig. 12iii there is a constant trend with extracted power values around 10 J/s, in Fig. 12i in phase of compression of the air trapped in the U-OWC chamber, the extracted power is lower than the air-decompression phase.

CONCLUSIONS

In this paper, a 2D CFD numerical model, implemented on the Ansys Fluent Software was validated, through a small-scale experimental campaign performed within a flume equipped with a U-OWC device, scaled with respect to the REWEC device installed in NOEL laboratory in Reggio Calabria.

To validate the numerical model, experimental and numerical tests were conducted, comparing the results of the free surface oscillation within the flume and inside the vertical duct of the U-OWC. A good agreement between the numerical and experimental results has been found. The validated numerical model was used to perform an analysis of the U-OWC's energy

balance as the incident wave parameters changed.

The energy results, obtained as the wave height and wave period vary, show:
• great values of the reflection coefficient (C_r) and reflected energy (E_R);
• small extracted energy (E_E) values from PTO system;
• great amounts of energy losses (E_L) due to turbulence and vortex within the U duct;
• small potential energy (E_S) values, due to the small amplitude of oscillation of the free surface inside the device.

In particular, it has been found that as the period of the incident wave decreases, the reflection in the caisson tends to increase, decreasing the efficiency of the caisson in terms of energy extracted from the PTO system.

While, as the wave height varies, maximum efficiency values were recorded in correspondence of an intermediate wave height value between the tests conducted.

Due to the large energy losses and high reflection values found in the tests performed when the parameters of incident wave were

changed, it was decided to perform an analysis of the energy balance as the geometrical parameters of the caisson varied. By varying the length and height of the U-OWC air chamber, the measurements of oscillation of the free surface, flow rate, air pressure oscillation and energy extracted from the PTO system were extrapolated from the validated numerical model.

From the results obtained, it is possible to state that:
• the oscillation of the free surface increases as the length of the air chamber decreases and the height of the air chamber increases. This trend determines maximum potential energy (P_E) values of the U-OWC in high and tight air chambers;
• the extracted energy (E_E) increases as the length of the air chamber decreases and the height of the air chamber increases;

• the extracted energy (E_E) remains constant during the compression and decompression of the air as the length of the air chamber changes, while, the energy extracted (E_E) is greater during the air compression phase for large values of height of air chamber.

The results obtained from the energy balance constitute a valid tool for defining the optimal shape and dimensions to be adopted in future experimental and numerical campaigns, in order to maximize the energy production of the device and minimize losses due to the formation of vortices. This campaign will be performed in the 18 m long wave flume of the Hydraulics Laboratory at the University of Messina (see e.g., FARACI, 2018 or FARACI et alii, 2019 for details).

REFERENCES

BAUDRY V., BABARIT A. & CLEMENT A., (2013) - *An overview of analytical, numerical and experimental methods for modelling oscillating water columns.* In: 10th European Wave and Tidal Energy Conference (EWTEC), September 2 - 5, Aalborg, Denmark.

BOCCOTTI P. (2002) - *Caisson for absorbing wave energy.* European patent ep n, 1133602 b1, usa patent n. 6450732 b1.

BOCCOTTI P. (2007) - *Comparison between a U-OWC and a conventional OWC.* Ocean Engineering, **34**: 799 - 805. doi:10.1016/j.oceaneng.2006.04.005.

BRUSCA S., CUCINOTTA F., GALVAGNO A., LANZAFAME R., MAURO S. & MESSINA M. (2015) - *Oscillating water column wave energy converter by means of straight-bladed darrieus turbine.* In Energy Procedia, **82**: 766 - 773. doi:10.1016/j.egypro.2015.11.809.

CONTESTABILE P., FERRANTE V., DI LAURO E. & VICINANZA D. (2017) - *Full-scale prototype of an overtopping breakwater for wave energy conversion.* Coastal Engineering Proceedings, **1** (35): 12. doi:10.9753/icce.v35.structures.12.

CREMA I., SIMONETTI I., CAPPIETTI L. & OUMERACI H. (2015) - *Laboratory experiments on oscillating water column wave energy converters integrated in a very large floating structure.* In: 11th European Wave and Tidal Energy Conference (EWTEC), September 6 - 11, Nantes, France.

DEAN R. G. & DALRYMPLE R. A. (1992) - *Water wave mechanics for engineers and scientists.* World Scientific, Singapore.

DREW B., PLUMMER A. R. & SAHINKAYA M. N. (2009) - *A review of wave energy converter technology. proceedings of the institution of mechanical engineers. part a.* Journ. Power Energy, **223** (8): 887 - 902.

FALCÃO A. F. (2010) - *Wave energy utilization: a review of the technologies.* Renewable & sustainable energy reviews, **14** (3): 899 - 918, doi:10.1016/j.rser.2009.11.003.

FALCÃO A. F. & HENRIQUES J. C., (2015) - *Oscillating-water-column wave energy converters and air turbine: a review.* Renewable Energy, **85**: 1391 - 1424.

FARACI C., SCANDURA P. & FOTI E. (2015) - *Reflection of sea waves by combined caissons.* Journal of Waterway, Port, Coastal and Ocean Engineering, **140** (5). doi:10.1061/(asce)ww.1943-5460.0000275.

FARACI C. (2018) - *Experimental investigation of the hydro-morphodynamic performances of a geocontainer submerged reef.* Journal of Waterway Port Coastal and Ocean Engineering, **144** (2). doi:10.1061/(asce)ww.1943-5460.0000434

FARACI C., SCANDURA P., PETROTTA C. & FOTI E. (2019) - W*ave-induced oscillatory flow over a sloping rippled bed.* Water, **11** (8): 1618.

FERREIRA F. B., FALCÃO D. S., OLIVEIRA V. B. & PINTO A. M. F. R. (2015) - *Numerical simulations of two-phase flow in proton exchange membrane fuel cells using the volume of fluid method - a review.* Journal of Power Sources, **277:** 329 - 342.

FILIANOTI P. & CAMPOREALE S. M. (2008) - A *linearized model for estimating the performance of sea wave energy converters.* Renewable Energy, **33**: 631 - 641. doi:10.1016/j.renene.2007.03.018

GALVIN C. J. (1964) - *Wave height prediction for wave generators in shallow-water.* U.S. Army Coastal Engineering Res. Center. Washington, D.C.

GODA Y. & SUZUKI Y. (1976). - *Estimation of incident and reflected waves in random wave experiments.* Proc., 15th Int. Coastal Engineering Conf., ASCE, 828 - 845, New York.

HIRT C. W., NICHOLS B. D. (1981) - *Volume of Fluid (VoF) method for the dynamics of free boundaries.* J. Comput. Phys., **39** (1): 201 - 225.

KO C. H., TSAI C. P., CHUANG C. Y. & CHEN Y. C. (2017) - *An experimental study of hydrodynamics of an improved owc converter.* In: 27th International Ocean and Polar Engineering Conference, San Francisco, California.

LIANG C. & ZUO L. (2017) - *On the dynamics and design of a two-body wave energy converter.* Renewable Energy, **101**: 265 - 274. doi:10.1016/j.renene.2016.08.059.

LIU Y. & FARACI C. (2014) - *Analysis of orthogonal wave reflection by a caisson with open front chamber filled with sloping rubble mound.* Coastal Engineering, **91**: 151 - 163.

Lopez I., Andreu J., Ceballos S., Martinez De Alegría I. & Kortabarria I. (2013) - *Review of wave energy technologies and the necessary power equipment.* Renewable and Sustainable Energy Reviews, **27**: 413 - 434.

Luo Y., Nader J. R., Cooper P. & Zhu S. P. (2014) - *Nonlinear 2D analysis of the efficiency of fixed oscillating water column wave energy converters.* Renewable Energy, **64**: 255 - 265.

Malara G., Romolo A., Fiamma V. & Arena F. (2017) - *On the modelling of water column oscillations in U-OWC energy harvesters.* Renewable Energy, **101**: 964 - 972.

Mansard E. P. D. & Funke E. R. (1980) - *The measurement of incident and reflected spectra using a least squares method.* Proc., 17th Int. Coastal Engineering Conference, ASCE, 154 - 172, New York.

Moñino A., Medina - Lopez E., Clavero M. & Benslimane S. (2017) - *Numerical simulation of a simple owc problem for turbine performance.* International Journal of Marine Energy. doi:10.1016/j.ijome.2017.11.004.

Naty S., Viviano A. & Foti E. (2016) - *Wave energy exploitation system integrated in the coastal structure of a mediterranean port.* Sustainability. Multidisciplinary Digital Publishing Institute, **8** (12): 1342.

Scarpetta F., Torresi M., Camporeale S. M. & Filianoti P. F. (2017) - *CFD simulation of the unsteady flow in an oscillating water column: comparison between numerical and experimental results for a small scale experimental device.* Proc., 15th Int. European Wave and Tidal Energy Conference, Aug 27 - Sept 1, Cork, Ireland.

Simonetti I., Cappietti L., El Safti H. & Oumeraci H. (2015) - *Numerical modelling of fixed oscillating water column wave energy conversion devices: toward geometry hydraulic optimization.* (OMAE2015-42056). In: ASME 2015 34th International Conference on Ocean, Offshore and Arctic Engineering, May 31 - June 5, St. John's, Newfoundland, Canada.

Tseng R. S., Wu R. H. & Huang C. C. (2000) - *Model study of a shoreline wave-power system.* Ocean Engineering, **2**: 801 - 882.

Vicinanza D., Contestabile P., Nørgaardb J. & Andersenb T. L. (2014) - *Innovative rubble mound breakwaters for overtopping wave energy conversion.* Coastal Engineering, **88**: 154 - 170.

Zhang Y., Zou Q. P. & Greaves D. (2012) - *Air-water two-phase flow modelling of hydrodynamic performance of an oscillating water column device.* Renewable Energy, **41**: 159 - 170.